

Spin-Orbit Splittings between $2p_{3/2}$ - $2p_{1/2}$ and $1f_{5/2}$ - $1f_{7/2}$ Neutron States in ^{40}Ca , ^{38}Ar , ^{36}S and ^{34}Si N = 20 Isotones with Covariant Density Functionals

K. Karakatsanis¹, G.A. Lalazissis¹, P. Ring², E. Litvinova^{3,4}

¹Physics Department, Aristotle University of Thessaloniki,
Thessaloniki GR-54124, Greece

²Physik Department, Technische Universität München,
D-85747 Garching, Germany

³Department of Physics, Western Michigan University,
Kalamazoo MI 49008-5252 USA

⁴National Superconducting Cyclotron Laboratory, Michigan State University,
East Lansing, MI 48824-1321, USA

Abstract. One of the most successful ways of studying nuclear structure phenomena throughout the whole nuclide chart, has been the use of self-consistent mean field models. One of the most important advantages of relativistic mean-field (RMF) models in nuclear physics is the fact that the large Spin-Orbit (SO) potential emerges automatically from the inclusion of Lorentz-scalar and -vector potentials in the Dirac equation [1]. It is therefore of great importance to compare the results of such models with those of non-relativistic models and with experimental data.

1 Introduction

There has been lately a renewed interest in studies concerning the spin orbit part of the nuclear force. On the experimental level, inspired by the identification of ^{34}Si as a bubble nucleus which is due to the central depletion in the proton density (see Figure 1), an effect that is attributed to the removal of two protons from the $2s_{1/2}$ proton state, a very specific experiment by Burgunder et.al. was carried out [2]. Using a target of ^{35}Si and measuring the spectroscopic factors and the gamma spectrum of a (d,p) transfer reaction they were able to determine the energies of the first excited neutron states $1f_{7/2}$, $2p_{3/2}$, $2p_{1/2}$ and $1f_{5/2}$. The important result was a significant reduction in the $2p$ splitting between ^{36}S and ^{34}Si , which can be used as a further constraint on the strength of the Spin-Orbit force in various mean field models.

On the theoretical level, based on the aforementioned experiment there has been a study within the non-relativistic mean field approach [3]. Using various

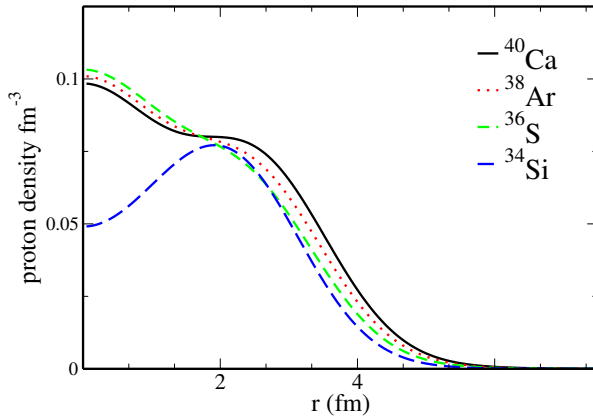


Figure 1. Proton density of the ^{40}Ca , ^{38}Ar , ^{36}S and ^{34}Si with DD-ME2.

Skyrme and Gogny functionals they analyse the 2p and 1f neutron spin-orbit splittings in the $N = 20$ isotones ^{40}Ca , ^{36}S and ^{34}Si . Our goal is to see how are the various nonlinear and density dependent covariant density functionals, compare with these experimental and theoretical results.

Subsequently we are concerned with the same $N=20$ nuclei ^{40}Ca , ^{36}S and ^{34}Si . Concentrating on the first 1f7/2, 2p3/2, 2p1/2 and 1f5/2 neutron states, we calculate the SO splittings of the 2p and 1f orbitals, using a Relativistic Hartree Bogolyubov (RHBS) code with spherical symmetry, employing three general types of functionals:

Nonlinear: NL3, NL3*, FSUGold.

Density dependent meson exchange: DD-ME2, DD-ME δ

Density dependent point coupling: DD-PC1, PC-PF1

Our investigation is carried out in three steps. On the first step we calculate the neutron single particle energies solving the Relativistic Dirac Hartree equations, without the inclusion of any pairing scheme. This will give us the pure relativistic mean field effect on the spin-orbit splittings.

On the second step we explore the effect of pairing which is expected to have an impact since, apart from ^{40}Ca , the nuclei we are dealt with are open shell in the proton channel. For that end we use the Bogolyubov quasiparticle framework. The TMR pairing force [4] which is separable in momentum space and is fitted to reproduce the pairing gap of the Gogny force in symmetric nuclear matter, is used to determine the pairing interaction.

Finally we consider two specific extensions of the standard relativistic mean field approach. The first one has to do with the fact that in the functionals we have mentioned above there are no exchange or tensor terms. One way to

account for them is by introducing the One Pion Exchange Potential (OPEP), which has a tensor like nature. This has been done for the nonlinear case [5] and the parameter set NL3RHF2 that has been produced is the one we use for that kind of extension. The second extension we examine is the Particle Vibration Coupling (PVC) [6, 7]. It takes into account correlations between the two different areas of the energy spectrum, the discrete part of the bound states and the continuous part of collective low lying excitations. This is important in our case since these correlations produce a fragmentation of the bound states close to the Fermi surface, such as the ones we are studying.

2 Numerical Results

2.1 Pure mean-field effect

For the case of the pure mean field we show in Table 1, the percentage of the reduction in the $1f$ and $2p$ splittings. First as we go from ^{40}Ca to ^{36}S and then as we go from ^{36}S to ^{34}Si . In the last column we show the same results from the relative experimental studies of these nuclei see refs. [2, 9, 10].

Additionally in Figure 2, we have plotted collectively for every one of the models we implemented diagrams the evolution of the p (panel (I)) and f (panel (II)) splittings, with respect to the mass number A .

In this first approach we observe a small relative reduction in the f and p splittings as we move along from ^{40}Ca to ^{36}S . However when we move to ^{34}Si we have a large reduction for the p splitting between 40% and 60%.

A similar investigation has been carried out in Ref. [3] for the non-relativistic Skyrme SLy5 and Gogny D1S functionals and certain tensor extensions of them. For the pure mean-field level, the results are shown in Table 2. Again we see small reductions when we go from ^{40}Ca to ^{36}S in both SLy5 and D1S, but there is a difference with the relativistic cases when we go from ^{36}S to ^{34}Si . Namely the neutron f splitting gets reduced by 26% (20%) for the SLy5 (D1S) force, whereas for the relativistic cases we have very small reductions and the neutron

Table 1. Relative SO splittings reductions of f and p neutron states for the case of no pairing

		SO reduction from $^{40}\text{Ca} \rightarrow ^{36}\text{S}$						
	NL3	NL3*	FSUGold	DD-ME2	DD-Med	DD-PC1	PC-PF1	Exp.
f	11%	11%	13%	12%	9%	9%	9%	0.5%
p	-6%	-8%	5%	3%	13%	8%	-10%	0.4%
		SO reduction from $^{36}\text{S} \rightarrow ^{34}\text{Si}$						
	NL3	NL3*	FSUGold	DD-ME2	DD-Med	DD-PC1	PC-PF1	
f	5%	6%	6%	6%	6%	7%	6%	2%
p	61%	60%	54%	47%	40%	46%	57%	43%

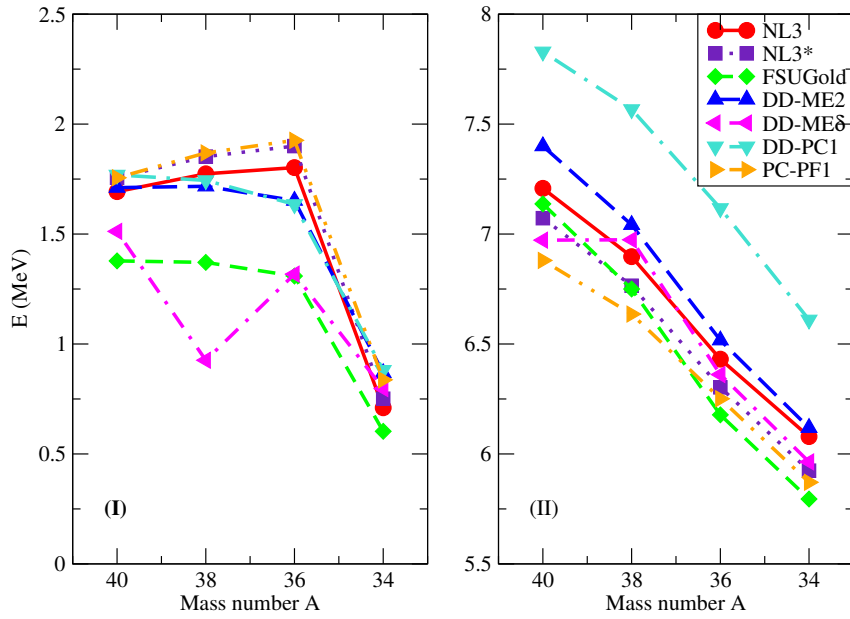


Figure 2. Evolution of Spin-Orbit p (panel (I)) and f (panel (II)) neutron splittings with respect to the mass number A , without pairing.

Table 2. Relative SO splittings reductions of f and p neutron states for the non-relativistic case as shown in Ref. [2]

Splitting	$^{40}\text{Ca} \rightarrow ^{36}\text{S}$		$^{36}\text{S} \rightarrow ^{34}\text{Si}$	
	f	p	f	p
SLy5	6%	8%	26%	40%
D1S	8%	13%	20%	43%
Exp.	0.5%	0.4%	2%	43%

p splitting has a reduction of about 40% which is the lowest we get with out including any pairing scheme.

2.2 The effect of pairing

In Table 3 we present the same SO splitting reductions but now for the case where pairing is included for the ^{38}Ar , ^{36}S and ^{34}Si proton subsystems. Likewise in Figure 3 in the top diagram there is the evolution of the $1f$ and $2p$ SO splittings for every parameter set and in the bottom diagram just for the NL3.

The SO splittings from these calculations are shown schematically in Figure 3 for all the forces collectively.

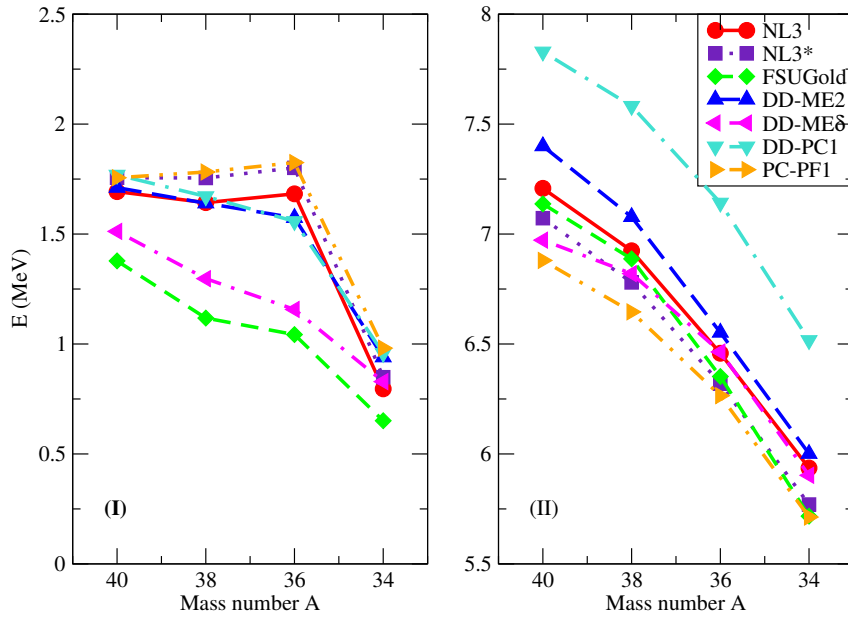


Figure 3. Same as Figure 2 but with TMR pairing.

 Table 3. Relative SO splittings reductions of f and p neutron states for the case of TMR pairing.

	NL3	NL3*	FSUGold	DD-ME2	DD-Med	DD-PC1	PC-PF1	Exp.
SO reduction from $40\text{Ca} \rightarrow 36\text{S}$								
f	10%	11%	11%	11%	7%	9%	9%	0.5%
p	1%	-3%	24%	8%	23%	12%	-4%	0.4%
SO reduction from $36\text{S} \rightarrow 34\text{Si}$								
f	8%	9%	10%	8%	9%	9%	9%	2%
p	53%	53%	38%	40%	28%	39%	46%	43%

We observe that with pairing included, we get lower reductions in the p splittings as we go from ^{36}S to ^{34}Si , as compared to the results without pairing. This is because the energy difference between $2p_{1/2} - 2p_{3/2}$ in ^{34}Si , is larger by 0.1MeV in all the functionals we use.

2.3 The case of tensor forces and Particle Vibrational Coupling model

In Table 4 we show the results we got with the nonlinear parameter set with the inclusion of one pion exchange. For comparison there are also the results of the similar investigation carried out in Ref. [3], with the parameter set SLy5T-2013 and D1ST2c-2013 that also include tensor terms in the total effective forces.

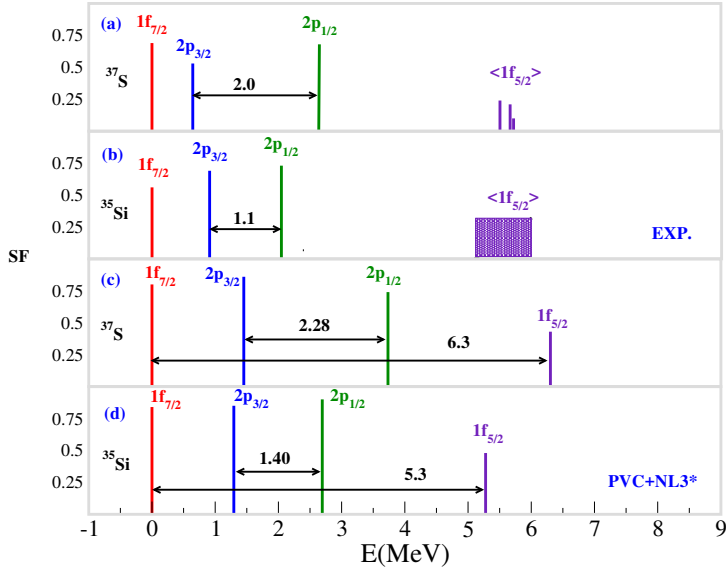


Figure 4. Distribution of the major fragments of the single particle strengths of ^{37}S (panel (a)) and ^{35}Si (panel (b)) as given in ref. [2] and the same distribution calculated with PVC for the force.

Table 4. Spin-orbit splittings reductions of f and p states for the case of tensor forces we also show for comparison the results from Ref. [3]

	$^{40}\text{Ca} \rightarrow ^{36}\text{S}$		$^{36}\text{S} \rightarrow ^{34}\text{Si}$	
	f	p	f	p
RHF2 with NL3	26%	14%	12%	60%
SLy5 $_T$ -2013	18%	39%	20%	43%
D1ST $_{2c}$ -2013	18%	27%	16%	42%
Exp.	0.5%	0.4%	2%	43%

What we see is that the inclusion of one pion exchange as an effective tensor force leads to an enhancement of the quenching of the spin-orbit splitting of the p states

Finally in Figure 4 we compare the results from the PVC calculations for ^{37}S and ^{35}Si with experimental results of Ref. [2]. More specifically, we show the position of the major fragments and the splittings between the f and p states as well as their spectroscopic factors. The experimentally observed reduction is 43% for the p states. It is in rather good agreement with the results obtained from the theoretical PVC calculations, which show a reduction of 39%. In both cases these are the splittings for the major fragments.

3 Conclusion

In general we can reproduce the qualitative picture of the experiment which means that we observe the relatively unchanged size of all the SO splittings except for a large reduction in of the $2p_{3/2}$ - $2p_{1/2}$ neutron states as we go from ^{36}S to ^{34}Si . Quantitatively for that specific case, for the pure mean-field level all of the forces show a large reduction of 40-60% in the 2p orbitals. When we include pairing we see that the respective percentages are reduced. The implementation of tensor forces goes into the opposite direction, with a larger reduction than the calculations which include pairing forces for the NL3 functional. So this extension does not seem to improve in anyway our theoretical description. For the specific case of the NL3* with PVC instead, we see that the relative reduction $2p_{3/2}$ - $2p_{1/2}$ neutron states is even more decreased and is lower from the results we got with our pairing scheme. Suggesting that the general property of this model, that leads to a smaller gap and a more dense spectrum near the Fermi surface, is a more reasonable extension for this kind of measurements.

Acknowledgements

This research is funded by the Greek State Scholarship Foundation (IKY), through the program “IKY Fellowships of excellence for postgraduate studies in Greece”, by the DFG cluster of excellence “Origin and Structure of the Universe” (www.universe-cluster.de), and by US-NSF grant PHY-1404343.

References

- [1] H.-P. Dürr, *Phys. Rev.* **103** (1956) 469.
- [2] G. Burgunder, O. Sorlin, F. Nowacki, S. Giron, F. Hammache, M. Moukaddam, N. de Séréville, D. Beaumel, L. Caceres, E. Clément, G. Duchêne, P. Ebran, J.B. Fernandez-Dominguez, F. Flavigny, S. Franchoo, J. Gibelin, A. Gillibert, S. Grévy, J. Guillot, A. Lepailleur, I. Matea, A. Matta, L. Nalpas, A. Obertelli, T. Otsuka, J. Pancin, A. Poves, R. Raabe, A. Scarpaci, J.I. Stefan, C. Stodel, T. Suzuki, and C. Thomas, *Phys. Rev. Lett.* **112** (2014) 042502.
- [3] M. Grasso and M. Anguiano, *Phys. Rev. C* **92** (2015) 054316.
- [4] Y. Tian, Z. Y. Ma, and P. Ring, *Phys. Lett. B* **676** (2009) 44.
- [5] G.A. Lalazissis, S. Karatzikos, M. Serra, T. Otsuka, and P. Ring, *Phys. Rev. C* **80** (2009) 041301.
- [6] E. Litvinova and P. Ring, *Phys. Rev. C* **73** (2006) 044328.
- [7] E. Litvinova, P. Ring, and V.I. Tselyaev, *Phys. Rev. C* **75** (2007) 064308.
- [8] G.A. Lalazissis, S. Karatzikos, R. Fossion, D. Peña Arteaga, A.V. Afanasjev, and P. Ring, *Phys. Lett. B* **671** (2009) 36.
- [9] Y. Uozumi, N. Kikuzawa, T. Sakae, M. Matoba, K. Kinoshita, S. Sajima, H. Ijiri, N. Koori, M. Nakano, and T. Maki, *Phys. Rev. C* **50** (1994) 263.
- [10] G. Eckle, H. Kader, H. Clement, F. Eckle, F. Merz, R. Hertenberger, H. Maier, P. Schiemenz, and G. Graw, *Nucl. Phys. A* **491** (1989) 205.

K. Karakatsanis, G.A. Lalazissis, P. Ring, E. Litvinova

- [11] S.A. Changizi, C. Qi, and R. Wyss, *Nucl. Phys. A* **940** (2015) 210.
- [12] W. Satuła, J. Dobaczewski, and W. Nazarewicz, *Phys. Rev. Lett.* **81** (1998) 3599.
- [13] A.H. Wapstra, G. Audi, and C. Thibault, in *Nucl. Phys. A* **729** (2003) 129, the 2003 NUBASE and Atomic Mass Evaluations.